WARSAW UNIVERSITY OF TECHNOLOGY Index 351733
FACULTY OF CIVIL ENGINEERING
COMMITTEE FOR CIVIL AND WATER ENGINEERING
POLISH ACADEMY OF SCIENCES ISSN 1230-2945

DOI: 10.24425/ace.2026.1399

ARCHIVES OF CIVIL ENGINEERING

Vol. LXXII ISSUE 3 2026

pp. 385 – 399

Research paper

A study on cage design and material utilization analysis of builders hoist

Youcun Fang[1], Chujie Jiang[2], Rui Tian[3]

Abstract: Builders hoist is an important transport equipment in high-rise buildings, and the material of the cage accounts for a large proportion of builders hoist, and the unreasonable distribution of the cage components will greatly cause material redundancy. In order to reduce the production cost of builders hoist and maximize the material utilization rate, the static analysis and finite element calculation of the cage of builders hoist are carried out by ANSYS Workbench, and the topology optimization and response surface method are used to carry out the secondary lightweight design and modal analysis of the cage. The results show that the optimised cage structure layout is more reasonable, meets the requirements of mechanical properties and strength, and does not resonate, and the mass is reduced by 489 kg, with a weight reduction ratio of 40.75%, and the light weighting effect is remarkable.

Keywords: builders hoist, lightweight design, modal analysis, response surface method, topology optimization

[1]MSc., Lec., School of Mechanical and Electrical Engineering, Guangdong Construction Polytechnic, Guangzhou 510440, China, e-mail: fyc2024@yeah.net, ORCID: 0009-0002-9913-3665
[2]Bac., Eng., Guangzhou Tewei Eng. Machinery Co., Ltd, Guangzhou 5100080, China, e-mail: jcj1980@yeah.net, ORCID: 0009-0006-7355-7362
[3]MSc., Sr. Eng, School of Mechanical and Electrical Engineering, Guangdong Construction Polytechnic, Guangzhou 510440, China, e-mail: tianrui0711@163.com, ORCID: 0009-0000-8950-3795

1. Introduction

Builders hoists, or construction elevators, are essential for vertical transport in high-rise building construction, moving materials, equipment, and personnel between floors. Fixed to the hoisting platform, they allow vertical cage movement along guide rails, enhancing construction efficiency, especially in tall buildings where cranes and manual methods are inadequate [1]. There are two main types: rack and pinion SC series, favored for stability, safety, and energy efficiency, and steel wire rope SS series. With the global focus on green, low-carbon development, manufacturers must innovate, improving performance, reducing costs, and simplifying processes. Lightweight design is crucial, cutting material use, boosting energy efficiency, and lowering carbon footprints [2].

The cage, a primary load-bearing component, accounts for about one-fifth of the hoist's total mass. Its design and material distribution significantly affect weight and performance. Inefficient designs can lead to material redundancy, increasing cost and weight without proportional strength or safety benefits. Thus, optimizing the cage's design for strength, weight, and material efficiency is a key research area [3]. This paper focuses on lightweight SC builders hoist cage design using topology optimization and the response surface method (RSM). Topology optimization determines optimal material distribution within a design space, reducing weight while maintaining structural integrity. RSM models and analyzes relationships between input variables and output responses. Combining these methods aims for a lightweight cage design meeting mechanical properties and safety standards [4]. Static and modal analyses ensure design reliability. Static analysis assesses the cage's response to static loads, while modal analysis evaluates dynamic behavior, including natural frequencies and mode shapes, to identify resonance issues and ensure operational load withstanding [5].

2. Lightweight design methods and processes

2.1. Research status

Lightweight design optimizes parts/assemblies for structural strength and rigidity by selecting proper cross-sections or adjusting structural layouts. This optimizes size, shape, and structure, minimizing material use for a lightweight structure and reducing manufacturing costs. Lightweighting includes three approaches: lightweight structure, process, and materials [5]. Structural optimization is widely accepted for improving performance and reducing material use and costs. The earliest application was in automobile frame design. Studies include: Yoo et al. [6] proposing a multi-resolution topology optimization method to enhance car body torsional stiffness; Shin K-S et al. [7] conducting multi- objective function topology optimization of automobile material density for overall frame performance; Simon Š et al. [8] focusing on car mass reduction with bending stiffness and torsional strength as primary conditions for car body topology optimization.

Topology optimization optimizes material size, shape, structure, and distribution in a given area based on constraints, loads, and other indicators [9]. Significant progress has been made in computational analysis, especially in determining the best component layout through finite element method analysis [10]. It focuses on stiffness maximization (flexibility minimization) for a single load case to find the optimal material distribution. Compared to traditional size optimization, it offers more design freedom [11] and is a promising structural material design method.

The response surface method is a common structural optimization technique that establishes a correlation model between input and response variables for optimization. Many scholars have applied it to various structures. For example, Xu et al. [12] used ANSYS for static analysis and optimized a sinkhole boring machine's slewing device, reducing its mass. Zhang et al. [13] used the finite element method for static analysis and proposed a structural optimization scheme for a gantry bending machine. Ding et al. [14] optimized CSG dam parameters and calculated the optimal cross- section. Xing et al. [15] constructed a response surface model for a downhole cyclone separator, improving its separation efficiency through structural optimization.

2.2. Lightweight design process based on topology optimization-response surface method

Determine the initial values and value intervals of the design variables according to the actual situation of the SC-type builders hoist cage, Parametric 3D modelling of the builders hoist cage by SolidWorks software, and import it into ANSYS Workbench for static analysis to obtain the lightweight margin information of the builders hoist cage; adopt the mathematical model based on the variable-density SIMP interpolation to optimize the topology and secondary design of the cage; adopt the central composite design; adopt the central composite test to optimize the structure of the cage and the secondary design; adopt the response surface model to optimize the structure of the cage; and adopt the response surface model to optimize the structure of the cage. The topology optimization and secondary design of the cage are carried out based on the mathematical model of variable density SIMP interpolation method; the sample points are collected by the central composite test design method and the response values of the sample points are obtained by using finite element numerical simulation technology; the response surface model of tthe builders hoist cage frame mass and the maximum equivalent force is constructed based on the data of the sample points; finally, the static analysis and modal analysis are carried out for the cage after the light-weighting design.

3. Static analysis of the cage

3.1. Finite element modelling

Depending on the solid structural form of the SC builders hoist cage, through SolidWorks software to establish the cage three-dimensional model, imported into ANSYS Workbench to establish the finite element model, as shown in Fig. 1. Based on the actual project specifications, the cage material was set as structural steel with a modulus of elasticity (E) of 68.9 GPa, a Poisson's ratio (μ) of 0.33, and a density (ρ) of 2800 kg/m^3. The original weight of the cage is 1200 kg. To enhance the computational efficiency of the finite element model, geometric features such as process holes, welded joints, and smaller chamfered fillets, which have minimal influence on the overall mechanical properties, were omitted [16]. The finite element model was generated utilizing the meshing tool, with a cell size set to 50 mm, resulting in 100,146 nodes and 49,760 cells. For the design working condition, the maximum average load capacity of the cage was considered. The cage was constrained in the X, Y, and Z directions on the upper face, and in the X and Y directions on the lower face. Additionally, a maximum working load of 15,000 N was uniformly applied to the upper surface of the lower part of the cage, as depicted in Fig. 2.

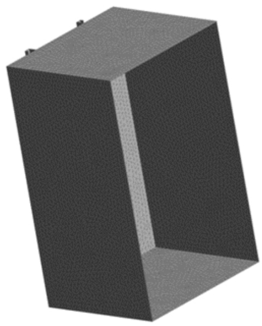

Fig. 1. Finite element model of cage

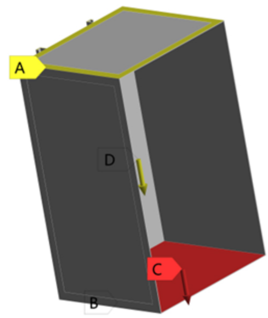

Fig. 2. Boundary condition setting of cage

3.2. Static analyses

The static analysis shows that the maximum deformation of the cage is 14.1 mm, and the maximum strain is 0.0004 mm/mm, this strain value is insignificant in comparison to the overall dimensions of the cage, indicating that the cage's design satisfies the stiffness criteria. Furthermore, the maximum stress of the cage is 69.419 MPa, which is smaller than the bending ultimate strength of structural steel 230 MPa, therefore, the design of the cage meets the strength requirements and has a lot of lightweight design space, as shown in Fig. 3.

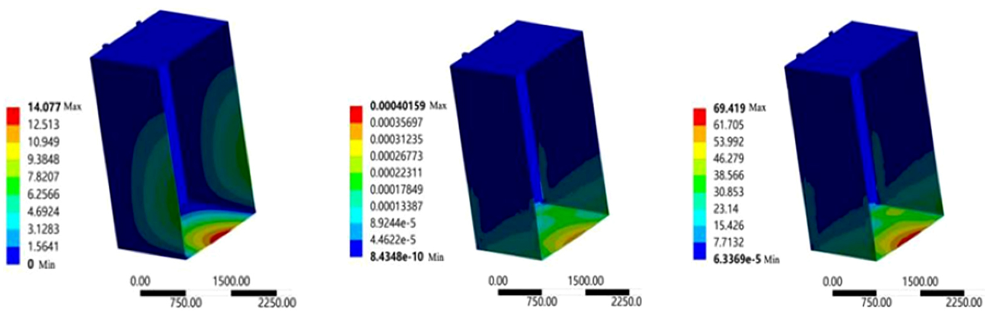

(a) (b) (c)

Fig. 3. Results of cage static analysis; (a) Deformation maps, (b) Strain maps, (c) Maximum stress maps

4. Optimisation of the overall topology of the cage

4.1. Establishment of mathematical model for topology optimisation

In the mathematical modelling of cage topology optimisation, a mathematical model based on variable density SIMP interpolation [17–19] is used: the relative density of each cell of the structure is set as the design variable and the minimum flexibility of the structure is taken as the objective function. The mathematical model is as follows Eq. (4.1):

$$\left\{\begin{array}{rl} \text{Find} & \rho = (\rho_1, \ldots, \rho_n) \\ \min & c(\rho) = \boldsymbol{u}^T \boldsymbol{K} \boldsymbol{u} = \sum_{e=1}^{n} (\rho_e)^p \boldsymbol{u}_e^T \boldsymbol{K}_e \boldsymbol{u}_e \\ \text{Subject to} & \boldsymbol{K}(\rho)\boldsymbol{u} = \boldsymbol{P} \\ & V(\rho) \le 0.9 \cdot V_0 \\ & 0 < \rho_{\min} \le \rho_i \le 1 \end{array}\right. \tag{4.1}$$

where: ρ – the relative density of the material, $c(\rho)$ – structural suppleness, p is the penalty factor, $p > 1$, $\boldsymbol{u}$ – the displacement vector at each node of the finite element model, $\boldsymbol{K}$ – the overall structural stiffness matrix, $\boldsymbol{u_e}$ – the displacement vector of the unit node, $\boldsymbol{K_e}$ – the unit stiffness matrix, $\boldsymbol{P}$ – the load vector, $V(\rho)$ – the volume after structural optimization, V_0 – the volume before optimization, $\rho_{\min}$ – the minimum relative density value of the material.

4.2. Topology optimisation process

Without changing the cage assembly principle and satisfying the maximum stiffness objective, the design region and exclusion region are set, the material-based density is selected for topology optimisation [20], the response type is selected for compliance, the maximum number of iterations is 500, and the mass is used as the response with a retention percentage of 60%, as shown in Fig. 4. After 12 optimisation iterations, the optimisation result is mainly to remove the less stressed areas of the cage while retaining the more stressed areas, which is in accordance with the basic principle of optimisation, as shown in Fig. 5.

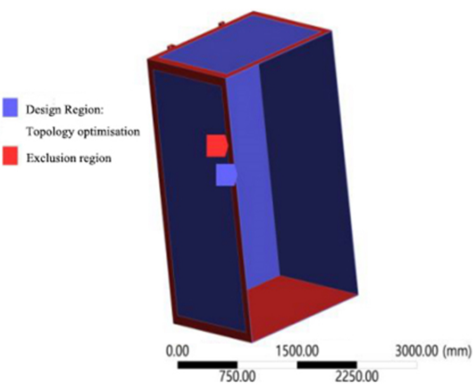

Fig. 4. Topology optimisation restriction region

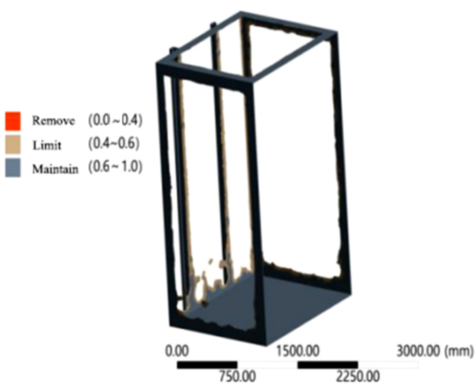

Fig. 5. Topology optimisation resultant surface

Under the premise of not changing the cage assembly principle and meeting the maximum stiffness target, the design area and exclusion area are set. Solid Isotropic Material with Penalization (SIMP) interpolation method based on material density was adopted for topology optimization [20]. In this process, the detailed Settings are as follows: Select compliance as the response type, set the maximum number of iterations to 500, take quality as the response variable, and set the volume retention percentage after structure optimization to 60%. In addition, in order to ensure the accuracy of the optimization results, density filtration technology with a filter radius of 30 mm was used to avoid checkerboard phenomenon, and the movement limit was set to 1.5 to smooth the boundary changes during the optimization process. After 12 optimization iterations, the optimization results mainly removed the low-stress region of the cage, while retaining the high-stress region, which conforms to the basic principle of optimization, as shown in Figure 5.

4.3. Secondary design of topology optimisation model

Although topology optimization design can effectively reduce the structural weight and enhance performance, the optimization results often exhibit complex morphologies that can be challenging to process. Consequently, a secondary design phase is necessary to ensure compliance with production standards and actual manufacturing requirements [21]. After thoroughly considering the actual manufacturing process, material properties of the structure, structural strength and stiffness analysis, as well as the assembly and maintenance characteristics of the cage structure, the cage's mass following the secondary design is 1000.4 kg, representing a 16% weight reduction. This outcome aligns with the demands of engineering practice and exhibits improved industrial production capability and operability, as depicted in Fig. 6.

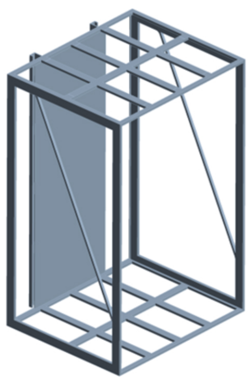

Fig. 6. Secondary modelling after cage topology optimization

5. Cage frame response surface optimisation

Response Surface Methodology (RSM) is a modelling method that adopts the experimental design theory to test the specified design points to obtain the response surface model of the response about the design variables and use it to predict the response values of the non-sample points, which is able to reflect the relationship between the response and the design variables more realistically in the design space and has the advantages of easy calculation and easy iteration [22, 23]. It is easy to calculate and easy to iterate. Therefore, the lightweight design of cage frames based on the response surface model can greatly improve the optimisation efficiency and ensure the accuracy of the optimisation results.

5.1. Establishment of response surface model

The cage frame of builders hoist is mainly welded by channel steel, angle steel and so on, take the left ($P1$) right ($P2$) lower ($P3$) upper ($P4$) frame wall thickness of the cage as the optimization design variables, and establish the second-order polynomial response surface model to optimize the cage frame structure, Eq. (5.1).

$$y(X) = a_0 + \sum_{i=1}^{n} a_i x_i + \sum_{i=1}^{n} a_{ii} x_i^2 + \sum_{i=2}^{n} \sum_{j=1}^{i-1} a_{ij} x_i x_j \tag{5.1}$$

where: $y(X)$ is the response variable, in this paper, the response variable is the mass of the cage, the maximum equivalent force and the maximum deformation; a_0, a_i, a_{ii}, a_{ij} are the coefficients to be determined; n refers to the number of input variables; x_i, x_j are the input data.

It is obvious that the model of the second-order response surface has a total number of coefficients to be determined, these coefficient values can be ascertained using the least squares method. The quadratic polynomial response surface model of Eq. (5.1) can be written in the form of a matrix, as shown in Eq. (5.2).

$$Y = Xa + \varepsilon \tag{5.2}$$

where: Y is the response matrix,$Y = (y_1, y_2, \ldots, y_n)^T$; a is the matrix of coefficients to be determined,$a = (a_1, a_2, \ldots, a_k)^T$; ε is the error term, $\varepsilon = (\varepsilon_1, \varepsilon_2, \ldots, \varepsilon_k)^T$; k is the number of experimental data; $X = \begin{bmatrix} 1 & \chi_{11} & \cdots & \chi_{1n} \\ 1 & \chi_{21} & \cdots & \chi_{2n} \\ \vdots & \vdots & \ddots & \vdots \\ 1 & \chi_{n1} & \cdots & \chi_{nn} \end{bmatrix}$.

Solved by the least squares method, the matrix of coefficients to be determined *can* be simplified to Eq. (5.3).

$$a = \left(X^T X\right)^{-1} X^T Y \tag{5.3}$$

$$Y \approx Xa \tag{5.4}$$

Eq. (5.4) is an approximate expression for the response surface to approximate the response values in the design domain, and Eq. (5.4) is obtained by substituting Eq. (5.3) into Eq. (5.2).

5.2. Experimental design

The selection of test sample points is crucial for the accuracy of the established response surface model; poorly chosen test points may even render the construction of the response surface model infeasible. Hence, it is imperative to judiciously determine the test points based on experimental design theory, ensuring they adequately cover the entire design space. The central composite design conducts numerical tests at both the center point and its extension points, guaranteeing test consistency. Moreover, the number of tests in this method facilitates an overall experimental design that tends towards orthogonality, aiding in the determination of the optimal configuration. Consequently, this study employs the central composite design to ascertain the test points.

The wall thickness of the left ($P1$) right ($P2$) lower ($P3$) upper and ($P4$) frames of the cage is considered as the optimization design variable, with a range of 10 mm to 28 mm. The design points are generated using the Mid-Latin Hypercube sampling method [24,25]. Through computation in ANSYS, 25 sets of design points are produced, and the response value for each sample point is obtained via finite element numerical simulation, as presented in Table 1.

Table 1. A simple longtable example

No.	$P1$ (mm)	$P2$ (mm)	$P3$ (mm)	$P4$ (mm)	Quality (tonne)	Maximum total deformation (mm)	Maximum equivalent force (MPa)
1	14.68	19.72	18.28	25.48	0.8073	7.2731	93.685
2	19	13.96	20.44	26.92	0.81231	5.8285	82.359
3	11.08	12.52	25.48	24.04	0.77467	3.7263	61.697
4	21.16	21.16	19.72	21.16	0.85225	5.6521	79.983
5	13.24	11.8	11.8	15.4	0.68613	22.318	191.29
6	26.92	20.44	22.6	24.76	0.9079	4.0387	63.667
7	18.28	21.88	13.96	27.64	0.82587	11.836	127.48
8	16.84	26.2	27.64	11.08	0.87259	2.7153	50.684
9	25.48	26.92	16.84	12.52	0.87594	6.7873	90.683
10	13.96	25.48	10.36	22.6	0.78876	23.006	266.15
11	20.44	10.36	15.4	14.68	0.73923	11.173	123.75
12	11.8	27.64	12.52	16.12	0.78274	15.422	197.04
13	17.56	15.4	24.04	26.2	0.83026	4.0481	64.674
14	10.36	18.28	26.92	13.24	0.78599	3.1536	54.778
15	23.32	16.12	26.2	20.44	0.86602	3.1827	55.282
16	19.72	23.32	16.12	13.96	0.81807	8.4373	103.5

Continued on next page

Table 1 – *Continued from previous page*

No.	*P*1 (mm)	*P*2 (mm)	*P*3 (mm)	*P*4 (mm)	Quality (tonne)	Maximum total deformation (mm)	Maximum equivalent force (MPa)
17	22.6	11.08	14.68	11.8	0.74575	11.9	126.9
18	21.88	22.6	23.32	16.84	0.87321	3.8908	62.528
19	27.64	17.56	13.24	17.56	0.8252	12.418	152.51
20	12.52	24.04	21.88	23.32	0.8354	4.7026	70.234
21	16.12	14.68	11.08	19	0.72776	22.713	196.24
22	24.76	19	17.56	21.88	0.85102	7.0445	92.677
23	26.2	16.84	19	19.72	0.84798	6.0654	82.115
24	15.4	13.24	24.76	10.36	0.76557	3.8998	63.246
25	27.001	10.049	10.172	27.219	0.78263	26.003	303.14

5.3. Response surface optimisation

Latin hypercube sampling involves drawing Q uniform sample data points within the range of 0 to 1 in an N-dimensional vector space. The matrices A and B, both of dimension $N \times Q$, are utilized to store the coordinates of these samples, respectively. The four design variables of the cage frame, namely $P1$, $P2$, $P3$, and $P4$, serve as input variables. The response values encompass the maximum equivalent force, mass, and maximum deformation of the cage under limit operating conditions. To fit the response surface to the output quantities, a non-parametric regression method is employed, which boasts high robustness, high model accuracy, and resistance to the influence of noise points. The established response surface model is illustrated in Fig. 7.

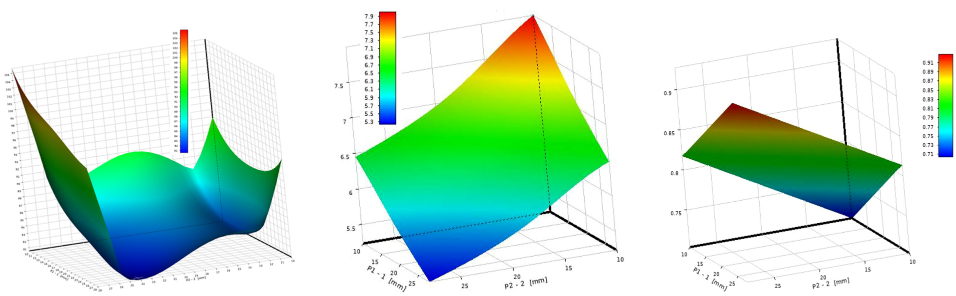

(a) (b) (c)

Fig. 7. Response surface model; (a) Equivalent stress surface diagram (b) Deformation response surface (c) Mass response surface

The optimisation objective function is set as the maximum equivalent stress is less than or equal to 100 MPa, the maximum deformation is less than 10mm, and the optimal three candidate points are selected. Combined with the actual production requirements, the candidate point 1 is selected as the final optimisation result, and the final result is optimised to be 10 mm for $P1$, 14 mm for $P2$, 22 mm for $P3$, and 17 mm for $P4$, and the mass of the optimised cage model is 711.7 kg, as shown in Table 2.

Table 2. Optimal three sets of candidate points

Candidate point	Group 1	Group 2	Group 3
$P1$ (mm)	10.011	10.025	10.038
$P2$ (mm)	14.502	21.252	11.127
$P3$ (mm)	22.002	24.002	26.002
$P4$ (mm)	17.202	10.722	21.522
Quality (tonne)	0.74374	0.77974	0.75577
Maximum total deformation (mm)	5.3618	4.058	3.4752
Maximum equivalent force (MPa)	73.169	62.797	68.324

6. Static and modal analysis of optimised cage

6.1. Static analysis of optimised cage

In order to verify whether the optimised cage meets the design requirements [26], the static analysis of the optimised cage is re-conducted according to the same material, the same mesh division, and the same boundary conditions as those of the pre-optimisation cage, and the optimisation results are shown in Fig. 8.

The changes in stress, deformation and mass of the cage before and after finishing optimisation are shown in Table 3.

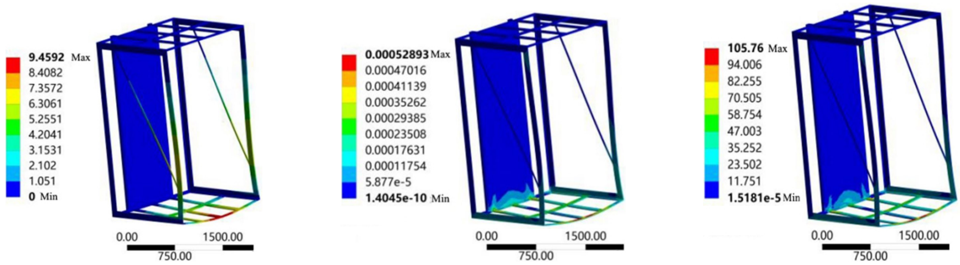

(a) (b) (c)

Fig. 8. Static analysis results of the optimised cage; (a) Deformation maps (b) Strain maps (c) Stress maps

Table 3. Comparison before and after cage optimisation

	Pre-Optimisation	Post-Optimisation	Variations
Maximum deformation (mm)	14.01	9.46	–4.55
Maximum stress (MPa)	69.42	105.76	36.34
Mass (kg)	1200	711.7	–489

After the cage optimisation, the maximum deformation is reduced by 4.55 mm, the maximum stress is increased by 36.34 MPa, but it is still smaller than the maximum permissible stress of 230 MPa of the material structural steel, and the mass is reduced by 489 kg, the weight reduction ratio reaches 40.75%, the result proves that the cage optimisation has a good effect of lightweighting.

6.2. Modal analysis of optimised cage

The electric motor is used as the power source of the construction lift, which is driven by rack and pinion meshing, and its excitation frequency is analysed as follows:

1. The intrinsic frequency of the three-phase asynchronous motor $f = 50$ Hz.
2. The installation height of the guide frame is 150 m, a total of 100 sections of the standard section in the cage up and down movement process, in the standard section and the standard section of the standard section connected to the roller vibration $n = 198$ times, when the cage running speed in the range of 20–63 m/min, the vibration frequency of the rollers generated $f = 0.44 - 1.386$ Hz.

Modal analysis of the cage after lightweight design is carried out to obtain the first six orders of intrinsic frequency and the vibration pattern at the corresponding frequency. The first six orders of intrinsic frequencies of the cage are shown in Table 4.

Table 4. Cage first six orders of intrinsic frequency

Ordinal number	Intrinsic frequency /Hz
first stage	7.31
second stage	9.35
third stage	9.56
fourth stage	13.06
fifth order	18.16
sixth order	19.17

The corresponding vibration pattern of the cage is shown in Fig. 9.

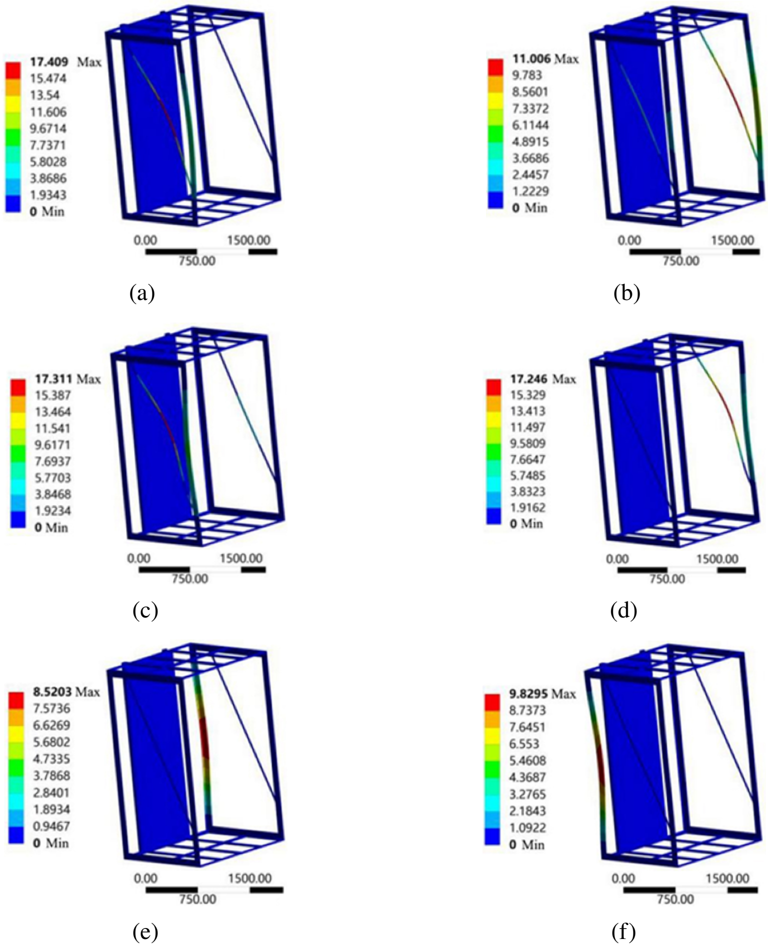

Fig. 9. The first six orders of vibration pattern of the cage; (a) First order, (b) Second order, (c) Third order, (d) Fourth order, (e) Fifth order, (f) Sixth order

The first six orders of the cage's intrinsic frequency are in the range of 7.31–19.17 Hz, which is much lower than the intrinsic frequency of the three-phase asynchronous motor, and much higher than the vibration frequency of the cage's rollers when they are rolling, so the external excitation of the motor and the rollers will not cause the cage to resonate.

6.3. Dynamic analysis of the optimised cage

To ensure the cage's reliability under real-world operating conditions, transient dynamic analyses were conducted to evaluate its response to impulse loads and varying payloads (empty and fully loaded states). The analysis focused on sudden acceleration/deceleration scenarios and collision events, which generate short-duration, high-magnitude forces.

(1) Finite Element Setup

Using ANSYS Workbench, transient dynamic simulations were performed with the following parameters: Empty load: Cage mass = 711.7 kg, payload = 0 kg.

Full load: Cage mass = 711.7 kg + maximum payload (15000 N ≈ 1530 kg).

Impulse load: A triangular pulse force of 20 kN (simulating abrupt stops) applied within 0.5 seconds.

(2) Results and Discussion

Empty vs. Full Load: The maximum deformation under full load increased by 12% compared to static analysis (from 9.46 mm to 10.59 mm), while stress remained below 120 MPa. The empty load showed negligible dynamic amplification.

Impulse Load Response: The peak equivalent stress reached 138 MPa, well below the material yield strength (230 MPa). The cage exhibited rapid damping of vibrations within 2 seconds, indicating stable dynamic behavior.

Fatigue Assessment: Miner's rule was applied to evaluate cumulative damage under cyclic impulse loads. Results confirmed a safety factor > 2.5 for a 10-year service life.

(3) Validation: Field tests with accelerometers installed on the cage validated the simulation results, showing a 5% deviation in vibration frequency and stress distribution.

7. Conclusions

The 3D model of an SC builders hoist cage was created using SolidWorks, and its finite element model was established in ANSYS Workbench for static analysis. Topology optimization and secondary design of the cage were conducted using a mathematical model based on the variable density SIMP interpolation method, reducing its weight by 199.6 kg (16%). A response surface model, established through Latin hypercubic sampling and non- parametric regression, further optimized the cage, achieving a total weight reduction of 489 kg (40.75%).

This paper's innovation lies in combining topological optimization and the response surface method for the lightweight design of building elevator cages, ensuring reduced weight without compromising mechanical properties, strength, or causing resonance. The optimization's reliability was verified through static and modal analyses. Focusing on the SC construction crane cage, this research achieved significant lightweight results. The methods and ideas are also applicable to other construction machinery, such as tower cranes, crawler cranes, and concrete pump trucks, which often have material distribution and structural redundancy issues. Extending these methods to these fields can enhance performance, reduce waste and costs, and promote green, low-carbon development in the construction machinery industry. Future studies can explore these methods' application in other machinery to increase results' value and comprehensiveness.

Acknowledgement

This study is supported by Special Fund Project of Science and technology innovation strategy of Guangdong Province (pdjh2024b565); Enterprise horizontal development project (2023101992).

References

[1] X. Shao, "Structural analysis and optimization for Builders Hoist", M.A. thesis, Chang'an University, China, 2016.

[2] T. Kim, H. Lim, S.W. Kim, H. Cho, and K. Kang, "Inclined construction hoist for efficient resource transportation in irregularly shaped tall buildings", *Automation in Construction*, vol. 62, pp. 124–132, 2016, doi: 10.1016/j.autcon.2015.11.008.

[3] N. Lu and X. Liu, "Control Strategy of Elevator Driving Device Based on Particle Swarm Optimization", *Science Technology and Engineering*, vol. 23, no. 26, pp. 11203–11205, 2023.

[4] F. Liu, "Lightweight Research on construction hoist", M.A. thesis, Chang'an University, China, 2018.

[5] F. Feppon, G. Allaire, C. Dapogny, and P. Jolivet, "Body- fitted topology optimization of 2D and 3D fluid-to-fluid heat exchangers", *Computer Methods in Applied Mechanics and Engineering*, vol. 376, art. no. 113638, 2021, doi: 10.1016/j.cma.2020.113638.

[6] J. Yoo, I.G. Jang, and I. Lee, "Multi-resolution topology optimization using adaptive isosurface variable grouping (MTOP-aIVG) for enhanced computational efficiency", *Structural and Multidisciplinary Optimization*, vol. 63, no. 4, pp. 1743–1766, 2021, doi: 10.1007/s00158-020-02774-2.

[7] H. Li, et al., "Three-dimensional topology optimization of a fluid-structure system using body-fitted mesh adaption based on the level- set method", *Applied Mathematical Modelling*, vol. 101, pp. 276–308, 2022, doi: 10.1016/j.apm.2021.08.021.

[8] S. Šilih, Z. Kravanja, and S. Kravanja, "The MINLP Approach to Topology, Shape and Discrete Sizing Optimization of Trusses", *Applied Sciences*, vol. 12, no. 3, art. no. 1459, 2022, doi: 10.3390/app12031459.

[9] S. Dou, "A projection approach for topology optimization of porous structures through implicit local volume control", *Structural and Multidisciplinary Optimization*, vol. 62, no. 2, pp. 835–850, 2020, doi: 10.1007/s00158-020-02539-x.

[10] P. Kumar, R.A. Sauer, and A. Saxena, "On topology optimization of large deformation contact-aided shape morphing compliant mechanisms", *Mechanism and Machine Theory*, vol. 156, art. no. 104135, 2021, doi: 10.1016/j.mechmachtheory.2020.104135.

[11] S. Das and A. Sutradhar, "Multi-physics topology optimization of functionally graded controllable porous structures: application to heat dissipating problems", *Materials & Design*, vol. 193, art. no. 108775, 2020, doi: 10.1016/j.matdes.2020.108775.

[12] GY Xu, ZC Qi, Y Z Tian, "Optimization design of rotary device of caisson roadheader based on response surface method", *Journal of Machine Design*, vol. 39, Supplement 2, pp. 92–97, 2022, doi: 10.13841/j.cnki.jxsj.2022.s2.021.

[13] K.T. Zhang, D.Z. Guan, S.W. Bai, and Z.G. Liu, "Lightweight design of gantry bending machine based on response surface methodology", *Manufacturing Automation*, vol. 41, no. 1, pp. 57–60, 2019.

[14] Z. Ding, J. Xue, X. Zhu, and J. Wang, "Optimization of CSG dam profile based on response surface methodology", *Case Studies in Construction Materials*, vol. 17, art. no. e01430, 2022, doi: 10.1016/j.cscm.2022.e01430.

[15] L. Xing, J.Y. Li, L.X. Zhao, M. Jiang, and G. Han, "Structural optimization of downhole hydrocyclones based on response surface methodology", *China Mechanical Engineering*, vol. 32, no. 15, pp. 1818–1826, 2021, doi: 10.3969/j.issn.1004-132X.2021.15.007.

[16] G.L. Bluhm, O. Sigmund, and K. Poulios, "Internal contact modeling for finite strain topology optimization", *Computational Mechanics*, vol. 67, no. 4, pp. 1099–1114, 2021, doi: 10.1007/s00466-021-01974-x.

[17] L. Lin, Q. Wen, and C. Wang, "Structural topology optimization of circular saw blade", *Journal of Machine Design*, vol. 35, no. 6, pp. 24–28, 2018, doi: 10.13841/ j.cnki.jxsj.2018.06.004.

[18] O. Giraldo-Londoño and G.H. Paulino, "PolyStress: a Matlab implementation for local stress-constrained topology optimization using the augmented Lagrangian method", *Structural and Multidisciplinary Optimization*, vol. 63, no. 4, pp. 2065–2097, 2021, doi: 10.1007/s00158-020-02760-8.

[19] G.A. Da Silva, N. Aage, A.T. Beck, and O. Sigmund, "Local versus global stress constraint strategies in topology optimization: a comparative study", *International Journal for Numerical Methods in Engineering*, vol. 122, no. 21, pp. 6003–6036, 2021, doi: 10.1002/nme.6781.

[20] W. Zhen, Y. Hu, H. Yu, and S. Scherer, "LiDAR-enhanced Structure-from-Motion", in *2020 IEEE International Conference on Robotics and Automation (ICRA), Paris, France*. IEEE, 2020, pp. 6773–6779, doi: 10.1109/ICRA40945.2020.9197030.

[21] A. Alaswad, A.G. Olabi, and K.Y. Benyounis, "Integration of finite element analysis and design of experiments to analyse the geometrical factors in bilayered tube hydroforming", *Materials & Design*, vol. 32, no. 2, pp. 838–850, 2011, doi: 10.1016/j.matdes.2010.07.015.

[22] S.J.S. Chelladurai, K. Murugan, A.P. Ray, M. Upadhyaya, V. Narasimharaj, and S. Gnanasekaran, "Optimization of process parameters using response surface methodology: A review", *Materials Today: Proceedings*, vol. 37, Part 2, pp. 1301–1304, 2021, doi: 10.1016/j.matpr.2020.06.466.

[23] V. Panwar, D.K. Sharma, K.V.P. Kumar, A. Jain, and C. Thakar, "Experimental investigations and optimization of surface roughness in turning of en 36 alloy steel using response surface methodology and genetic algorithm", *Materials Today: Proceedings*, vol. 46, Part 15, pp. 6474–6481, 2021, doi: 10.1016/j.matpr.2021.03.642.

[24] M.C. Trinh and H. Jun, "Stochastic bending and buckling analysis of laminated composite plates using Latin Hypercube Sampling", *Engineering with Computers*, vol. 39, no. 2, pp. 1459–1497, 2023, doi: 10.1007/s00366-021-01544-y.

[25] M. Saraninezhad, M. Ramezani, and H. Falaghi, "Probabilistic assessment of wind turbine impact on distribution networks by using Latin Hypercube Sampling method", in *2022 9th Iranian Conference on Renewable Energy & Distributed Generation (ICREDG), Mashhad, Iran*. IEEE, 2022, pp. 1–7, doi: 10.1109/ICREDG54199.2022.9804513.

[26] X.X. Gao and N. Lu, "Structural Analysis of a Heavy-Duty Deck Erection Gantry under Full Load and Horizontal Lifting Conditions Based on Ansys Workbench", *Journal of Beijing University of Civil Engineering and Architecture*, vol. 37, no. 4, pp. 81–83, 2021, doi: 10.19740/j.2096-9872.2021.04.10.

Received: 2024-09-23, Revised: 2025-02-18